BNL-225896-2024-TECH
EIC-ADD-TN-092

# Optical properties of wigglers for EIC Ring Electron Cooler

S. Seletskiy

July 2024

Electron-Ion Collider

**Brookhaven National Laboratory**

**U.S. Department of Energy**

USDOE Office of Science (SC), Nuclear Physics (NP)

# DISCLAIMER

# Optical properties of wigglers for EIC Ring Electron Cooler

S. Seletskiy*[1], A. Fedotov[1], G. H. Hoffstaetter[2], D. Kayran[1], J. Kewisch[1], J. Unger[2],

[1]Brookhaven National Laboratory
[2]Cornell University

July 9, 2024

## 1 Introduction

Electron Ion Collider (EIC) requires cooling of protons at top energy (275 GeV) to achieve the average design luminosity. Such a cooler must be capable of counteracting an IBS-driven emittance growth in proton bunches. The Ring Electron Cooler (REC) is a candidate for the EIC top energy cooler.

The REC is a non-magnetized RF-based 150 MeV electron cooler, in which electrons are kept in the storage ring and re-utilized for several million turns. The REC is equipped with 18 damping wigglers, which keep electrons' emittance constant by counteracting both electrons' IBS and a proton-electron beam-beam scattering happening in the cooling section. These wigglers operate at a relatively low energy but must have a rather high field to provide the required radiation cooling of electrons. As a result of this unique range of parameters, the wigglers' optics exhibits interesting features

The actual design parameters of the wigglers will be finalized in the REC lattice optimization. For these studies we use tentative parameters listed in Table 1

*seletskiy@bnl.gov

Table 1: REC wigglers' parameters

| | |
|---|---|
| $\gamma$-factor | 293 |
| peak field ($B_0$) [T] | 2.4 |
| wiggler period ($\lambda$) [m] | 0.2 |
| number of periods ($N_p$) | 20 |

# 2 Equations of motion

We consider motion in the wiggler's reference frame, our $x$-axis is directed in the wiggling direction, $y$-axis is orthogonal to the wiggling plane and $z$ is the direction along the wiggler's axis. Then the motion equations are:

$$\begin{aligned} x'' &= -\frac{B_y}{B\rho} + y'\frac{B_z}{B\rho} \\ y'' &= \frac{B_x}{B\rho} - x'\frac{B_z}{B\rho} \end{aligned} \tag{1}$$

Equations (1) are valid in the approximation of $x' \ll 1$ and $y' \ll 1$. In the Appendix A we show that for our parameters Eqs. (1) hold true.

The current design of the REC lattice requires small $\beta$-function in the wiggling direction throughout the wiggler ($\beta_x \approx 30$ cm). Therefore, a wiggler with a field distribution, producing focusing in the wiggling direction, is needed. Below, we will consider motion for two examples of possible wiggler's fields.

## 2.1 Wiggler with sextupole field

A common representation of fields inside a wiggler with $x$-variation of $B_y$ field is [1]:

$$\begin{aligned} B_x &= \frac{k_x}{k_y} B_0 \sinh(k_x x) \sinh(k_y y) \sin(kz) \\ B_y &= B_0 \cosh(k_x x) \cosh(k_y y) \sin(kz) \\ B_z &= \frac{k}{k_y} B_0 \cosh(k_x x) \sinh(k_y y) \cos(kz) \end{aligned} \tag{2}$$

where $k = 2\pi/\lambda$, and geometric parameters $k_x$ and $k_y$ are related via $k_x^2 + k_y^2 = k^2$.

Formulas (2) represent a wiggler with the poles shaped to produce a parabolic dependence of $B_y$ on $x$ near the center of the wiggler. Thus, the additional focusing in the $x$ direction is happening due to a bunch going with

an offset through a sextupole-like field. We will discuss this in more details in the following sections.

Substituting Eq. (2) into Eq. (1) we get:

$$\begin{aligned} x'' &= -b\cosh(k_x x)\cosh(k_y y)\sin(kz) + y' b\tfrac{k}{k_y}\cosh(k_x x)\sinh(k_y y)\cos(kz) \\ y'' &= b\tfrac{k_x}{k_y}\sinh(k_x x)\sinh(k_y y)\sin(kz) - x' b\tfrac{k}{k_y}\cosh(k_x x)\sinh(k_y y)\cos(kz) \end{aligned} \tag{3}$$

where $b = \frac{B_0}{B\rho}$.

Below we will be making several assumptions to find an approximate analytic solution of Eq. (3). All the assumptions will be justified later on.

First, we consider the $x$-equation in Eqs. (3). We omit the second term ($y'$-term) in the $x$-equation, assuming that it is a small correction to a particle's trajectory. We further approximate $\cosh(k_x x) \approx 1 + k_x^2 x^2/2$ and $\cosh(k_y y) \approx 1$, again assuming that $y^2$ term in $\cosh(k_y y)$ expansion results in a negligible correction.Then, we get:

$$x'' = -b\sin(kz) - b\sin(kz)\frac{k_x^2 x^2}{2} \tag{4}$$

We notice that a solution of the equation $x''_w = -b\sin(kz)$, corresponding to a wiggler with no gradient, is given by:

$$x_w(z) = \frac{b}{k^2}\sin(kz) + x_w(0) + \left(x'_w(0) - \frac{b}{k}\right) z \tag{5}$$

Setting $x_w(0) = 0$ and $x'_w(0) = b/k$ we get for a fast oscillating part of the $x$-trajectory: $x_w(z) = \frac{b}{k^2}\sin(kz)$.

Next, we assume that the second right-hand-side term of Eq. (4) $f(x) = b\sin(kz)k_x^2 x^2/2$ is a small perturbation of $x_w(z)$. Therefore, we substitute $f(x)$ with $f(x) \approx \langle f(x_w)\rangle + \langle\frac{df(x_w)}{dx}\rangle x = 0 + \frac{b^2 k_x^2}{2k^2}x$, where averaging is performed over a wiggling period. As a result, Eq. (4) becomes:

$$x'' = -b\sin(kz) - \frac{b^2 k_x^2}{2k^2}x \tag{6}$$

Solution of Eq. (6) is given by:

$$\begin{aligned} x = \;& \tfrac{2bk^2}{2k^4 - b^2 k_x^2}\sin(kz) + x_0 \cdot \cos\left(\tfrac{bk_x}{\sqrt{2}k}z\right) + \\ & + \tfrac{\sqrt{2}k}{bk_x}\left(x'_0 - \tfrac{2bk^3}{2k^4 - b^2 k_x^2}\right)\sin\left(\tfrac{bk_x}{\sqrt{2}k}z\right) \end{aligned} \tag{7}$$

where $x_0 = x(0)$ and $x'_0 = x'(0)$. Since $b^2 k_x^2 \ll k^4$, we can further simplify Eq. (7):

$$x = \frac{b}{k^2}\sin(kz) + x_0 \cdot \cos\left(\frac{bk_x}{\sqrt{2}k}z\right) + \frac{\sqrt{2}k}{bk_x}\left(x'_0 - \frac{b}{k}\right)\sin\left(\frac{bk_x}{\sqrt{2}k}z\right) \qquad (8)$$

Equation (8) is the sought-for approximate analytic solution for the motion in the wiggling plane.

To find an equation of motion in $y$ direction we, first, approximate the $y$ differential equation in Eq. (3) with:

$$y'' = bk_x^2 xy\sin(kz) - bkx'y\cos(kz) \qquad (9)$$

Next, we substitute $x$ and $x'$ defined by Eq. (8) with $x'_0 = b/k$ into Eq. (9) and average all fast-oscillating terms over the wiggling period:

$$y'' + \frac{b^2}{2}\left(1 - \frac{k_x^2}{k^2}\right)y = 0 \qquad (10)$$

Solution of Eq. (10) is:

$$y = y_0\cos\left(\frac{b\sqrt{k^2 - k_x^2}}{\sqrt{2}k}z\right) + y'_0\frac{\sqrt{2}k}{b\sqrt{k^2 - k_x^2}}\sin\left(\frac{b\sqrt{k^2 - k_x^2}}{\sqrt{2}k}z\right) \qquad (11)$$

Equation (11) gives the approximate analytic solution for the motion in the plane orthogonal to the wiggling one.

Comparison of Eqs. (8) and (11) to numerical integration of Eq. (3) (see Fig. 1) shows a good agreement between the derived analytic approximation and the solution of the exact equations of motion. This validates the assumptions made in derivation of Eqs. (8) and (11).

## 2.2 Wiggler with quadrupole field

Another possible representation of a wiggler with focusing, which was considered for the REC, is given by:

$$\begin{aligned} B_x &= B_0\cos(k_q x)\sinh(k_q y) \\ B_y &= B_0\cosh(ky)\sin(kz) + B_0\sin(k_q x)\cosh(k_q y) \\ B_z &= B_0\sinh(ky)\cos(kz) \end{aligned} \qquad (12)$$

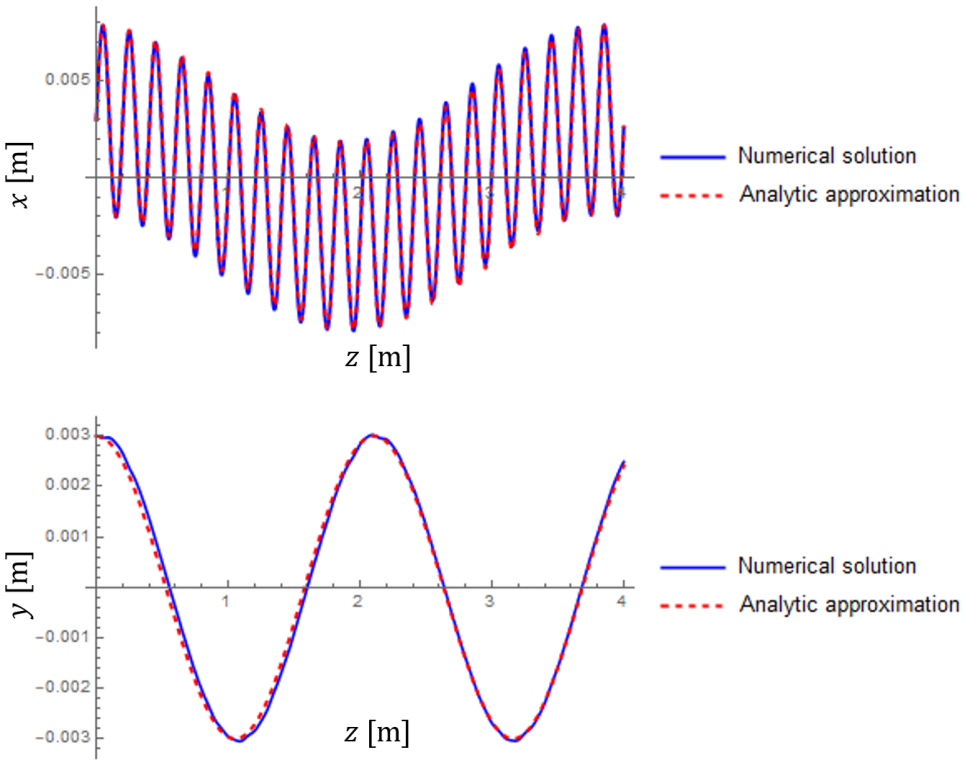


Figure 1: Numerical solution of equations of motion (3) and analytic approximations Eqs. (8), (11). The calculations are performed for $k_x = 15$ [m$^{-1}$] and $x_0' = b/k$.

Equations (12) correspond to a wiggler without gradient (represented by terms with $k$) inserted into a quadrupole (represented by terms with $k_q$), which provides focusing in $x$ direction.

Substituting Eq. (12) into Eq. (1) we get:

$$\begin{aligned} x'' &= -b(\cosh(ky)\sin(kz) + \sin(k_q x)\cosh(k_q y)) + y' b \sinh(ky)\cos(kz) \\ y'' &= b\cos(k_q x)\sinh(k_q y) - x' b \sinh(ky)\cos(kz) \end{aligned} \tag{13}$$

Next, we are employing the same assumptions that were made in Section 2.1 and we get the following approximate equations of motion:

$$\begin{aligned} x'' &= -b\sin(kz) - bk_q x \\ y'' &= (bk_q - x'bk\cos(kz))x \end{aligned} \tag{14}$$

A solution for $x$-equation in (14) is given by:

$$x = \frac{b}{k^2 - bk_q}\sin(kz) + x_0\cos(\sqrt{bk_q}z) + \left(x_0' - \frac{bk}{k^2 - bk_q}\right)\frac{\sin(\sqrt{bk_q}z)}{\sqrt{bk_q}} \tag{15}$$

Assuming that $b \ll k^2/k_q$, we get:

$$x = \frac{b}{k^2}\sin(kz) + x_0\cos(\sqrt{bk_q}z) + \left(x_0' - \frac{b}{k}\right)\frac{\sin(\sqrt{bk_q}z)}{\sqrt{bk_q}} \tag{16}$$

After substituting Eq. (16) into $y$-equation in (14), using $x_0' = b/k$, and averaging the fast-oscillating terms, we obtain:

$$y = y_0\cos\left(\sqrt{\frac{b^2}{2} - bk_q}z\right) + y_0'\frac{1}{\sqrt{\frac{b^2}{2} - bk_q}}\sin\left(\sqrt{\frac{b^2}{2} - bk_q}z\right) \tag{17}$$

Equations (16) and (17) represent an approximate analytic solution for the motion in the wiggler with quadrupole focusing.

Particle trajectories described by Eqs. (16) and (17) are in a good agreement with numerical integration of Eq. (13) (see Fig. 2).

# 3 Optical functions

In this section we will switch to the reference frame tied to a beam trajectory through the wiggler. Now, we will use symbols $x, x', y, y'$ to describe particles' motion in the trajectory frame and $\tilde{x}, \tilde{x}', \tilde{y}, \tilde{y}'$ to describe motion in the wiggler's frame. Although this switch makes things more confusing for a reader, it simplifies both the notations used below and the authors life.

## 3.1 Optical functions in a wiggler with sextupole field

First, we rewrite Eq. (8) in the new notations:

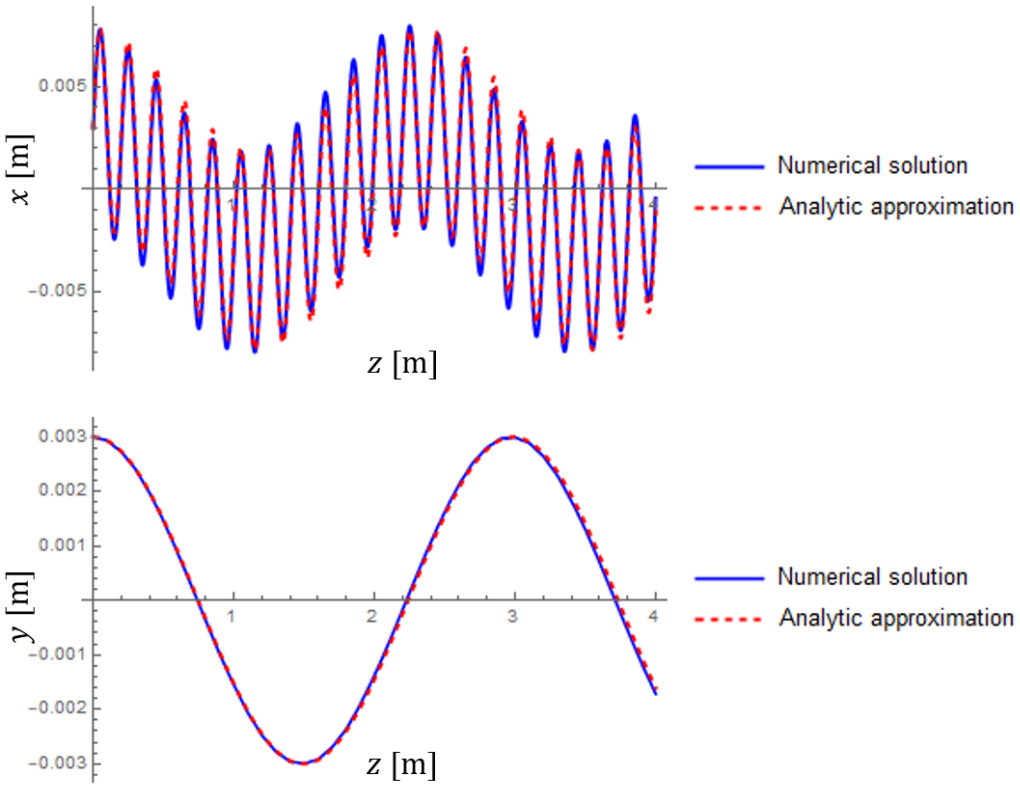


Figure 2: Numerical solution of equations of motion (13) and analytic approximations Eqs. (16), (17). The calculations are performed for $k_q = 1.5$ $[\mathrm{m}^{-1}]$ and $x_0' = b/k$.

$$\tilde{x} = \frac{b}{k^2}\sin(kz) + \tilde{x}_0 \cdot \cos\left(\frac{bk_x}{\sqrt{2}k}z\right) + \frac{\sqrt{2}k}{bk_x}\left(\tilde{x}_0' - \frac{b}{k}\right)\sin\left(\frac{bk_x}{\sqrt{2}k}z\right) \tag{18}$$

Then, the undisturbed beam trajectory in a wiggler is given by:

$$\tilde{x}_{ut} = \frac{b}{k^2}\sin(kz) - \frac{\sqrt{2}}{k_x}\sin\left(\frac{bk_x}{\sqrt{2}k}z\right) \tag{19}$$

Next, we observe that for our parameters the displacement $x$ in the trajectory frame is well approximated by a displacement $\hat{x}$ from $\tilde{x}_{ut}$ in the wiggler frame, as illustrated by Fig. 3. Indeed, simple considerations show that:

$$\begin{aligned} x &= \hat{x}\cos\left(\arctan\left(\tfrac{\partial\tilde{x}}{\partial z}\right)\right) = \hat{x}\cos\left(\arctan\left(\tfrac{b}{k}\cos(kz)\right)\right) \approx \\ &\approx \hat{x}\left(1-\tfrac{b^2}{2k^2}\cos^2(kz)\right) \end{aligned} \tag{20}$$

This shows that the difference between $x$ and $\hat{x}$ is less than $\approx 1\%$.

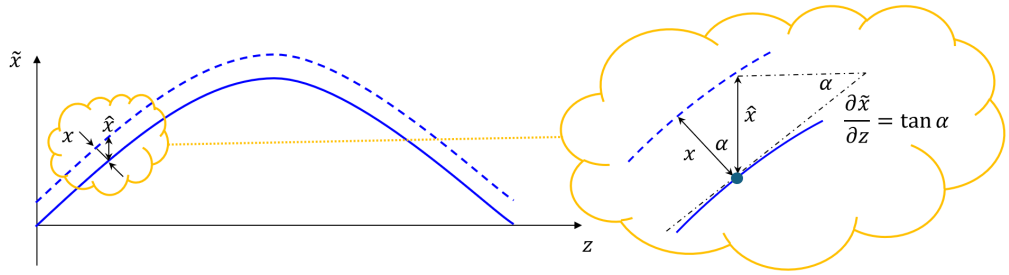


Figure 3: Relation between horizontal motion in the wiggler frame and the beam trajectory frame.

Finally, assuming $\tilde{x}_0 = x_0$ and $\tilde{x}'_0 = \frac{b}{k} + x'_0$, we get from Eq. (18):

$$x = x_0\cos\left(\frac{bk_x}{\sqrt{2}k}z\right) + x'_0\frac{\sqrt{2}k}{bk_x}\sin\left(\frac{bk_x}{\sqrt{2}k}z\right) \tag{21}$$

From Eq. (21) we obtain the transport matrix for a wiggling plane:

$$M_x = \begin{pmatrix} \cos\left(\frac{bk_x}{\sqrt{2}k}L\right) & \frac{\sqrt{2}k}{bk_x}\sin\left(\frac{bk_x}{\sqrt{2}k}L\right) \\ -\frac{bk_x}{\sqrt{2}k}\sin\left(\frac{bk_x}{\sqrt{2}k}L\right) & \cos\left(\frac{bk_x}{\sqrt{2}k}L\right) \end{pmatrix} \tag{22}$$

where wiggler's length $L = N_p\lambda$.

Similarly, for an orthogonal plane, Eq. (11) gives:

$$M_y = \begin{pmatrix} \cos\left(\frac{b\sqrt{k^2-k_x^2}}{\sqrt{2}k}L\right) & \frac{\sqrt{2}k}{b\sqrt{k^2-k_x^2}}\sin\left(\frac{b\sqrt{k^2-k_x^2}}{\sqrt{2}k}L\right) \\ -\frac{b\sqrt{k^2-k_x^2}}{\sqrt{2}k}\sin\left(\frac{b\sqrt{k^2-k_x^2}}{\sqrt{2}k}L\right) & \cos\left(\frac{b\sqrt{k^2-k_x^2}}{\sqrt{2}k}L\right) \end{pmatrix} \tag{23}$$

Equations (22) and (23) show that our wiggler is a thick lens. The matched beta-functions for such a wiggler are given by:

$$\beta_x = \frac{\sqrt{2}k}{bk_x}; \quad \beta_y = \frac{\sqrt{2}k}{b\sqrt{k^2 - k_x^2}} \tag{24}$$

From Eq. (25), the required $\beta_x = 30$ cm is achieved for $k_x = 30.9$ m$^{-1}$ (which gives $\beta_y = 1.6$ m). Notice that, for the parameters listed in Table 1, $k = 31.4$ m$^{-1}$. In other words, the needed focusing in the wiggling plane requires $k_x \to k$.

The phase advances in the wiggler are:

$$\phi_x = \frac{bk_x}{\sqrt{2}k} N_p \lambda; \quad \phi_y = \frac{b\sqrt{k^2 - k_x^2}}{\sqrt{2}k} N_p \lambda \tag{25}$$

From Eq. (25) number of betatron oscillations per wiggler depends on particle's relative momentum $\delta$ as:

$$\begin{aligned} Q_x &= \tfrac{1}{2\pi} \tfrac{b}{1+\delta} \tfrac{k_x}{\sqrt{2}k} N_p \lambda \approx \tfrac{1}{2\pi} \tfrac{bk_x N_p \lambda}{\sqrt{2}k} (1 - \delta) \\ Q_y &= \tfrac{1}{2\pi} \tfrac{b}{1+\delta} \tfrac{\sqrt{k^2 - k_x^2}}{\sqrt{2}k} N_p \lambda \approx \tfrac{1}{2\pi} \tfrac{b\sqrt{k^2 - k_x^2} N_p \lambda}{\sqrt{2}k} (1 - \delta) \end{aligned} \tag{26}$$

The resulting chromaticities are given by:

$$\begin{aligned} \eta_x &= \tfrac{\partial Q_x}{\partial \delta} = -\tfrac{1}{2\pi} \tfrac{B_0 N_p \lambda}{\sqrt{2} B\rho} \tfrac{k_x}{k} \\ \eta_y &= \tfrac{\partial Q_y}{\partial \delta} = -\tfrac{1}{2\pi} \tfrac{B_0 N_p \lambda}{\sqrt{2} B\rho} \tfrac{\sqrt{k^2 - k_x^2}}{k} \end{aligned} \tag{27}$$

This gives $\eta_x = -2.1$ and $\eta_y = -0.5$ for $k_x$ found above.

Equations (22)-(27) show that for the parameters of interest, when $k_x$ becomes close to $k$, $\eta_y \to 0$. So, with a limited contribution to chromaticity in a wiggling plane for each wiggler, wiggler's contribution to chromaticity in the orthogonal plane can be made negligibly small.

The dispersion in the wiggler is defined by Eq. (19) and, again assuming $\tilde{x}_0' = \frac{b}{k} + x_0'$, is given by:

$$D_x = -\frac{B_0}{k^2 B\rho} \sin(kz), \quad D_x' = -\frac{B_0}{kB\rho} \cos(kz) \tag{28}$$

Another observation is that for small $b = B_0/(B\rho)$, the wiggler becomes a short lens with average focusing parameters given by:

$$\langle K_x \rangle = \frac{B_0^2}{2(B\rho)^2} \frac{k_x^2}{k^2}, \quad \langle K_y \rangle = \frac{B_0^2}{2(B\rho)^2} \left(1 - \frac{k_x^2}{k^2}\right) \tag{29}$$

Equation (29) is a well known formula for wigglers operated at high energy, which provides $\langle K_x \rangle + \langle K_y \rangle = \frac{B_0^2}{2(B\rho)^2}$.

## 3.2 Optical functions in wiggler with quadrupole field

For the wiggler with quadrupole focusing (described in Section 2.2) we repeat the steps outlined in the previous section and obtain the following expressions for the transfer matrices:

$$M_{x1} = \begin{pmatrix} \cos\left(\sqrt{bk_q}L\right) & \frac{1}{\sqrt{bk_q}}\sin\left(\sqrt{bk_q}L\right) \\ -\sqrt{bk_q}\sin\left(\sqrt{bk_q}L\right) & \cos\left(\sqrt{bk_q}L\right) \end{pmatrix} \tag{30}$$

$$M_{y1} = \begin{pmatrix} \cos\left(\sqrt{\frac{b^2}{2} - bk_q}L\right) & \frac{1}{\sqrt{\frac{b^2}{2} - bk_q}}\sin\left(\sqrt{\frac{b^2}{2} - bk_q}L\right) \\ -\sqrt{\frac{b^2}{2} - bk_q}\sin\left(\sqrt{\frac{b^2}{2} - bk_q}L\right) & \cos\left(\sqrt{\frac{b^2}{2} - bk_q}L\right) \end{pmatrix} \tag{31}$$

From these equations, the matched beta-functions are given by:

$$\beta_{x1} = \frac{1}{\sqrt{bk_q}}; \quad \beta_{y1} = \frac{1}{\sqrt{\frac{b^2}{2} - bk_q}} \tag{32}$$

The phase advances in the wiggler are:

$$\phi_{x1} = \sqrt{bk_q}N_p\lambda; \quad \phi_{y1} = \sqrt{\frac{b^2}{2} - bk_q}N_p\lambda \tag{33}$$

The respective chromaticities are given by:

$$\begin{aligned} \eta_{x1} &= -\frac{\sqrt{B_0 k_q}N_p\lambda}{4\pi\sqrt{B\rho}} \\ \eta_{y1} &= -\frac{B_0 N_p\lambda}{2\pi\sqrt{2}B\rho}\frac{1-k_q B\rho/B_0}{\sqrt{1-2k_q B\rho/B_0}} \end{aligned} \tag{34}$$

According to Eqs. (32)-(34) the required $\beta_{x1} = 30$ cm corresponds to $k_q = 2.3$ m$^{-1}$, $\beta_{y1} = 1.6$ m, $\eta_{x1} = -1.1$ and $\eta_{y1} = -5.9$. So, in comparison to the wiggler with quadratic focusing, for the same $\beta$-functions the wiggler with linear focusing produces an order of magnitude larger chromaticity in $y$-plane.

This effect becomes more dramatic if one tries to make the focusing in the wiggling direction even tighter. Indeed, equating $\beta_x$ and $\beta_{x1}$ we get:

$$k_q = \frac{bk_x^2}{2k^2} \tag{35}$$

Therefore, from point of view of focusing properties of the wigglers, $k_x \to k$ is equivalent to $k_q \to b/2$. This means that while $\eta_y \to 0$ for the wiggler with quadratic focusing, for the linear focusing case $\eta_{y1} \to \infty$. We will discuss the physics behind this result in the next section.

Finally, once again, we notice that for the small parameter $b$:

$$\langle K_{x1} \rangle = bk_q, \quad \langle K_{y1} \rangle = \frac{b^2}{2} - bk_q \tag{36}$$

which gives $\langle K_{x1} \rangle + \langle K_{y1} \rangle = \frac{B_0^2}{2(B\rho)^2}$.

## 3.3 Chromaticities in case of strong focusing in wiggling direction

In Sections 3.1 and 3.2 we showed that in case of strong focusing in the wiggling direction, the chromaticity in the wiggling direction is limited for wigglers with both the quadratic and linear focusing. Yet, the chromaticities in the orthogonal direction exhibit very different behaviors. While for the wiggler with quadratic focusing the chromaticity in $y$-direction approaches 0, for the wiggler with linear focusing (producing the very same focal strength) $\eta_y \to \infty$. Let us explore what is behind this difference.

The equation of motion (1) for $y$ contains two terms, which have different physical meaning.

The term $x' \frac{B_z}{B\rho}$ represents a fringe focusing from wiggler's dipoles. Since, according to Maxwell's equations, fringes have a non-zero $B_z$ field, a particle with a non-zero $x'$ experiences a force in $y$ direction. In the wiggler with sinusoidal $B_y$ field, $B_z$ field must be sinusoidal as well. One can say that the wiggler introduces a "continuous edge effect" and therefore the focusing from $x' \frac{B_z}{B\rho}$ term is rather strong.

The term $\frac{B_x}{B\rho}$ represents an additional focusing due to a non-zero $B_x$ field. In our case it is a defocusing term, because we need focusing in $x$ direction.

Equations (8), (16) give the following expression for the beam trajectory through the wiggler (assuming $x_0 = 0,\ x_0' = b/k$):

$$x = \frac{b}{k^2}\sin(kz) \tag{37}$$

On the other hand, Eqs. (2), (12) show that for both types of considered wigglers:

$$B_z \approx y \cdot kB_0 \cos(kz) \tag{38}$$

Therefore, the "edge-focusing term" averaged over the wiggler's period provides:

$$\left\langle x' \frac{B_z}{B\rho} \right\rangle \approx y\langle b^2 \cos^2(kz)\rangle = y\frac{b^2}{2} \tag{39}$$

The additional defocusing (in $y$-direction) term $\frac{B_x}{B\rho}$ differs for the two types of wigglers.

For the wiggler with the fields given by Eq. (2), field $B_x$ can be approximated by:

$$B_x \approx y \cdot xk_x^2 B_0 \sin(kz) \tag{40}$$

Hence, the additional defocusing term for such a wiggler is:

$$\left\langle \frac{B_x}{B\rho} \right\rangle \approx y\langle xk_x^2 b \sin(kz)\rangle = y\left\langle \frac{k_x^2 b^2}{k^2}\sin^2(kz) \right\rangle = y\frac{b^2}{2}\frac{k_x^2}{k^2} \tag{41}$$

As Eqs. (39) and (41) show, for a wiggler with sextupole-like field both the edge-focusing and the additional focusing have the same dependence on $b$, that is the same dependence on a relative momentum offset $\delta$ for an off-momentum particle. This results in equation of motion (10): $y'' + \kappa_y^2 y = 0$ with $\kappa_y^2 = \frac{b^2(k^2-k_x^2)}{2k^2}$. Since the phase advance per wiggler is simply $\kappa_y L$, it is proportional to $b$ or to $(1+\delta)^{-1}$, which gives formulas (26) and (27). Therefore, as focusing in $y$-direction is getting zeroed ($\kappa_y \to 0$), in other words, as the motion in $y$-direction through the wiggler becomes equivalent to the motion in a drift, the chromaticity $\eta_y$ approaches zero.

For the wiggler with quadrupole focusing the situation is different. Equation (12) gives:

$$B_x \approx y \cdot k_q B_0 \tag{42}$$

Therefore, the additional focusing term for such a wiggler is:

$$\frac{B_x}{B\rho} = y \cdot k_q b \tag{43}$$

which means that the wiggler's edge-focusing term (39) depends on $\delta$ as $\propto (1+\delta)^{-2}$ while the additional focusing term has a dependence $\propto (1+\delta)^{-1}$. The respective equation of motion in $y$-direction is $y'' + \kappa_{y1}^2 y = 0$ with $\kappa_{y1}^2 = \frac{b^2}{2} - bk_q$. Then, the wiggler's chromaticity $\eta_{y1} = \frac{L}{2\pi}\frac{\partial \kappa_{y1}}{\partial \delta}\Big|_{\delta=0}$ is given by Eq. (34). This means that as $\kappa_{y1} \to 0$, the chromaticity in $y$-direction $\eta_{y1} \to \infty$.

Figure 4 shows the plots of $y$-chromaticities in the wigglers with two types of additional focusing considered above.

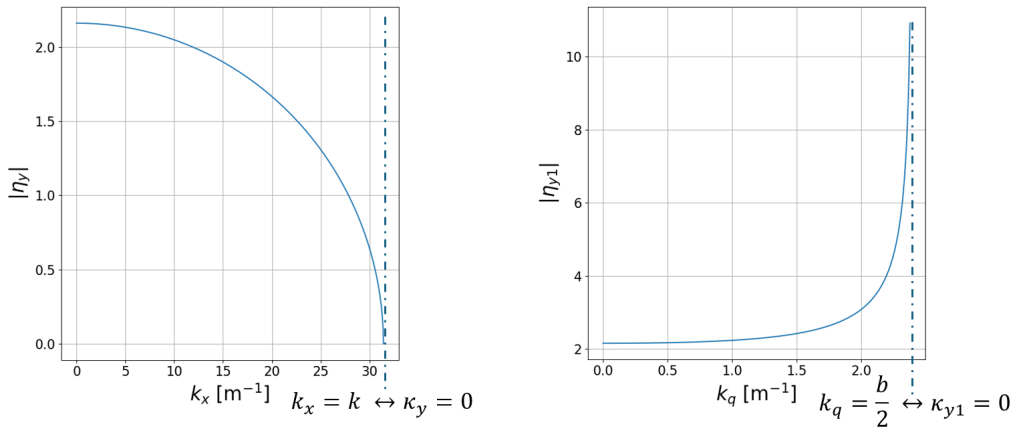


Figure 4: $y$-chromaticity in a wiggler with the sextupole-like (left plot) and quadrupole (right plot) additional focusing.

# 4 Conclusion

The EIC Ring Electron Cooler utilizes 4 meter long wigglers with high field and at a relatively low beam energy ($b = \frac{B_0}{B\rho} = 4.8$ m$^{-1}$). We showed that such a wiggler works as a thick lens in both the wiggling plane and the orthogonal one. The phase advance through these wigglers is substantial. As a result, one has to pay a special attention to the choice of additional focusing inside the wiggler, so that the wiggler's contribution to chromaticity is kept small.

We derived explicit analytic formulas for chromaticities of the wigglers with two possible field configurations.

For the wiggler with a sextupole field (2), where an additional focusing is provided by a beam moving with an offset in each pole, the contributions to chromaticities in both planes are small (27).

For the wiggler where focusing is provided by a quadrupole field (12) the chromaticity in the plane orthogonal to the wiggling plane becomes infinitely large as the focusing in that plane is approaching zero (34).

Since the Ring Electron Cooler lattice requires wigglers with a strong focusing in the wiggling plane and preferably zero focusing in the orthogonal plane, we need to make the wiggler's field as close as possible to the field given by Eq. (2).

# References

[1] R. P. Walker, Wigglers, ST-M-94-4, CERN (1993). https://cds.cern.ch/record/399409/files/p807.pdf

# A Exact and approximate equations of motion

In this section we are considering whether Eqs. (1), which assume small $x'$ and $y'$ are applicable to our parameters. The equations of motion obtained directly from Lorentz force and Newton's equations are:

$$\begin{aligned} x'' &= \frac{\sqrt{1+x'^2+y'^2}}{B\rho}\left[y'B_z - B_y - x'(x'B_y - y'B_x)\right] \\ y'' &= \frac{\sqrt{1+x'^2+y'^2}}{B\rho}\left[x'B_z - B_x - y'(x'B_y - y'B_x)\right] \end{aligned} \tag{44}$$

For $x' \ll 1,\ y' \ll 1$ Eqs. (44) becomes Eqs. (1).

Whether Eqs. (44) can be substituted with Eqs. (1) depends on how small $x'^2$ is, since for our wigglers $y'$ is obviously small.

Our first observation is that $\max(x') \approx b/k$ is probably a reasonable approximation. Then we can assume that throughout the wiggler $x'^2 \lesssim 0.02$, which suggests that a trajectory derived from Eqs. (1) must be a decent approximation of the actual physical trajectory through the wiggler.

To check whether a simple analytic expression (8) (derived from Eqs. (1)) is a valid simplification of Eqs. (44) we compare the trajectory given by Eq. (8) to the numerical solution of Eq. (44)) obtained for $x_0 = 0,\ x'_0 = -b/k,\ y_0 = 0,\ y'_0 = 0$ (see Fig. 5). The calculations were performed for $k_x = 30.9\ \mathrm{m}^{-1}$. It is worth mentioning that we checked that a similar level of agreement is achieved for both $k_x$ and $k$ being varied in a wide range.

Remembering that Eq. (8) is not an exact solution of Eqs. (1) but rather is an approximation, it is interesting to compare numerical solutions of Eqs. (1) and (44). The agreement between trajectories obtained from these equations becomes even better (see Fig. 6).

By the way, a "slow" extra-wiggling of trajectory that we see in numerical solutions of Eqs. (1) and (44) comes from the fact that the "true" optimal entrance angle is not $x'_0 = b/k$ but rather is $x'_0 = (2bk^3)/(2k^4 - b^2k_x^2)$, as Eq. (7) shows.

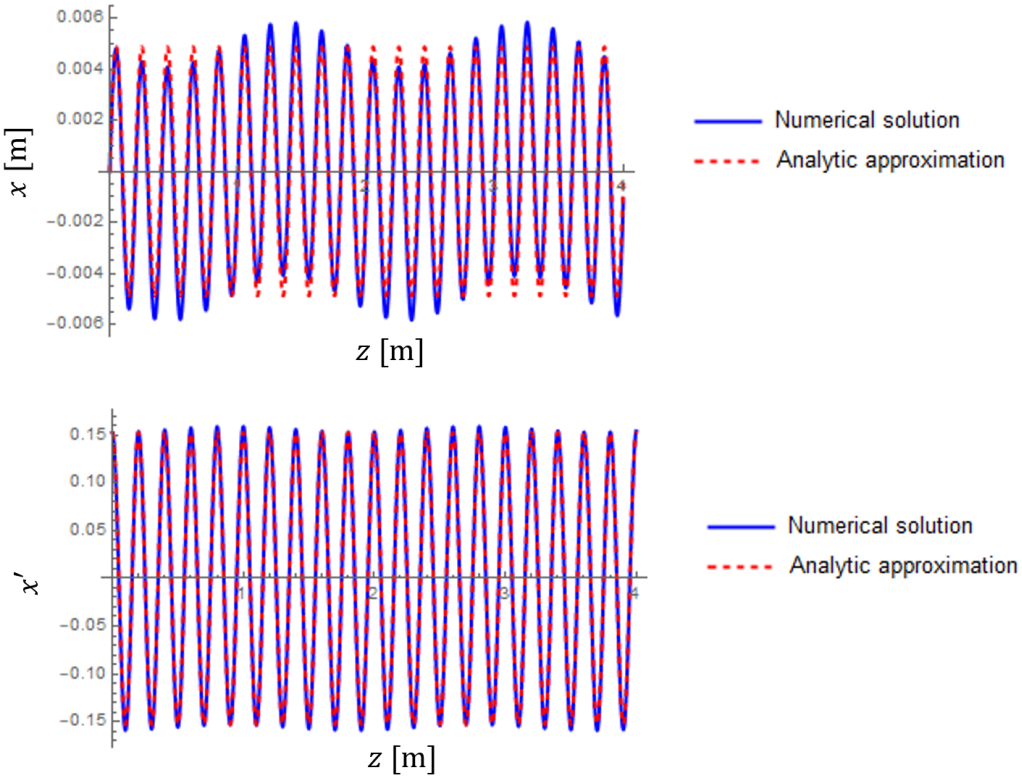


Figure 5: Comparison of numeric integration of Eq. (44) to an analytic trajectory given by Eq. (8).

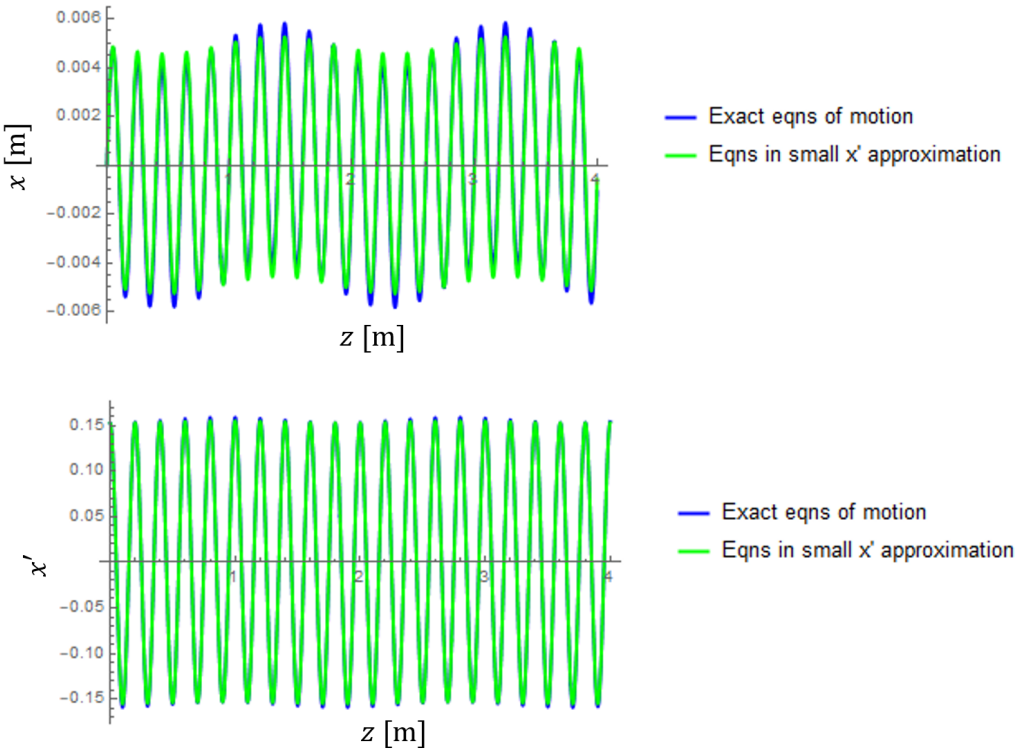


Figure 6: Comparison of numeric integration of exact equations of motion (44) and equations of motion (1).

# B Motion in case of $k_x > k$

For $k_x > k$ the fields (2) can be rewritten as:

$$\begin{aligned} B_x &= \tfrac{k_x}{\sqrt{k_x^2-k^2}} B_0 \sinh(k_x x) \sin(\sqrt{k_x^2-k^2}\, y) \sin(kz) \\ B_y &= B_0 \cosh(k_x x) \cos(\sqrt{k_x^2-k^2}\, y) \sin(kz) \\ B_z &= \tfrac{k}{\sqrt{k_x^2-k^2}} B_0 \cosh(k_x x) \sin(\sqrt{k_x^2-k^2}\, y) \cos(kz) \end{aligned} \tag{45}$$

Using the assumptions made in Section 2.1 we again can approximate fields (45) by:

$$\begin{aligned} B_x &\approx B_0 k_x^2 xy \sin(kz) \\ B_z &\approx B_0 k_z y \cos(kz) \end{aligned} \tag{46}$$

Also, we again obtain the trajectory in the wiggling plane:

$$\begin{aligned} x &\approx \tfrac{b}{k^2}\sin(kz) \\ x' &\approx \tfrac{b}{k}\cos(kz) \end{aligned} \tag{47}$$

Substituting Eqs. (46) and (47) into Eq. (1) and averaging over the fast oscillations in $x$, we get a familiar expression for $y$-motion:

$$y'' + \frac{b^2}{2}\left(\frac{k^2 - k_x^2}{k^2}\right) y = 0 \tag{48}$$

Equation (48) describes an oscillator for $k_x < k$, a motion in a drift for $k_x = k$, and an exponential growth for $k_x > k$, which is given by (assuming $y_0' = 0$):

$$y = y_0 \cosh\left(\frac{b\sqrt{k_x^2 - k^2}}{\sqrt{2}k} z\right) \tag{49}$$

To check the range of applicability of Eq. (49) we compare it to a numerical solution of Eq. (1) with the fields given by Eq. (45). Results of the comparison are shown in Fig. 7 .

As one can see, while $k_x$ is close to $k$ the analytic approximation (49) holds true. Yet, if we further increase $k_x$, the agreement with analytic approximation breaks down.

So, why is this happening? – This is happening because for an exponentially growing $y$ at some point $z_1$ along the wiggler the argument $y(z_1)\sqrt{k_x^2 - k_z^2}$ becomes so large that the linear expansion of cos and sin in Eq. (45) becomes invalid. Hence, a rule of thumb criteria for applicability of analytic Eq. (49) is:

$$y_0 \frac{\sqrt{k_x^2 - k^2}}{2} \exp\left(\frac{b\sqrt{k_x^2 - k^2}}{\sqrt{2}k} L\right) \lesssim \frac{\pi}{4} \tag{50}$$

For the case of REC wigglers we can assume $\beta_y \approx 3$ m inside the wiggler and $y$-emittance $\varepsilon_y \approx 8$ nm. It is reasonable to assume that the maximum $y_0 \approx 6\sqrt{\beta_y \varepsilon_y} \approx 1$ mm. Thus, as Fig. 7 shows, we expect Eq. (49) to be valid in the vicinity of $k_x = k$.

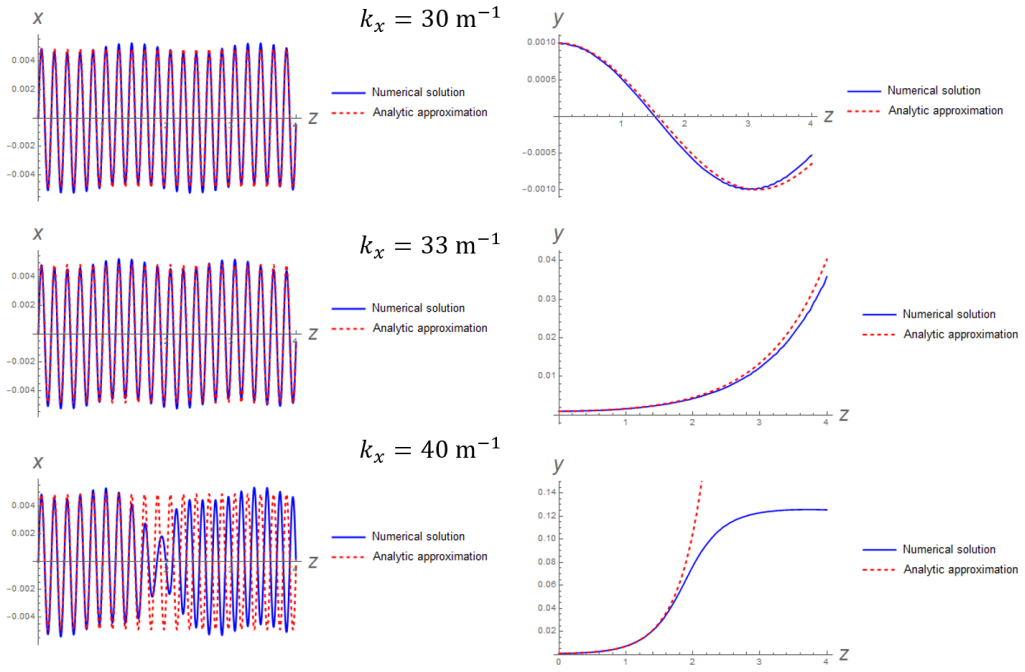


Figure 7: Numerical solution and an approximate analytic solution of the equations of motion for various $k_x$.